Engineering and Technology Journal
Journal homepage: https://etj.uotechnology.edu.iq

# Realization of an all-optical d and t flip flops with nano-structure using hybrid plasmonic waveguides



**Saif H. Abdulwahid**[a*], **Ahmed G. Waddday**[b], **Sinan M. Abdul Sattar**[a]

[a] Electrical Engineering Dept., University of Technology-Iraq, Alsina'a street, 10066 Baghdad, Iraq.
[b] Al-Furat Al-Awsat Technical University ATU, Kufa, Iraq.
*Corresponding author Email: eee.20.02@grad.uotechnology.edu.iq

## HIGHLIGHTS

- Optical D and T flip flops are designed using hybrid plasmonic waveguides
- The suggested design has nano dimensions of 400 $nm^2$
- There is an amplification effect in the Transmission values

## ARTICLE INFO

**Handling editor:** Makram A. Fakhri

**Keywords:**

Hybrid plasmonic waveguides
T and D flip flops
Square-shaped nano-ring resonators
Modulation depth
Contrast ratio

## ABSTRACT

Surface waves are electromagnetic waves propagating along the interface between a metal and an insulator. Surface waves break the diffraction limits and enable light to propagate in sub-wavelength structures. That opens the field of electro-opto devices. The main drawbacks of surface waves that move in the Plasmonic Waveguides (PWs) are propagation loss and low light confinement. Using a combination of the plasmonic waveguide and a Dielectric Waveguide (DW), the defect of the surface waves can be enhanced, and the Hybrid Plasmonic waveguide (HPW) is introduced. In this research, the design of an all-optical flip flop with 400 nm × 400 nm nano-scale dimensions, 1310 nm operating wavelength, and a transmission threshold ($T_{threshold}$) of 30% is shown using hybrid plasmonic waveguides (HPWGs) for Electro-Opto applications. It offers the basic structure for creating optical computers. The results of this structure are evaluated in a term of Contrast Ratio (CR), Modulation Depth (MD), and Insertion Losses (IL). The D-flip flop had an Insertion Loss of -1.4 dB, a CR of 7.45 dB, and a MD of 97.67%. The T-flip flop had an IL of -2.07 dB, a CR of 11.2 dB, and a MD of 95.29%. The mechanism that governs the operation of the suggested circuits depends on the constructive and destructive interferences between input ports and control ports. The simulation is based on the finite element method utilizing COMSOL software package version 5.5.

## 1. Introduction

As light waves interact with free electrons on a metal surface, specific surface waves are created at the interface between the two media [1-3]. These waves cause a phenomenon known as the surface plasmon polariton, which uses the basic functions of optical devices [4-7]. These surface waves can break the diffraction limit [8], allowing light to flow in waveguides of subwavelength dimensions.

The advantages and disadvantages of the plasmonic waveguides (PW) and the dielectric waveguides (DW) can be seen as one complete the other [9,10]. For example, DW can be regarded as a lossless guide, but there is a problem with the mode size. Conversely, PW can permit the light to flow under the diffraction limits, but there is a problem of high propagation loss. A great deal between confinement and propagation loss can be achieved by using a Hybrid Plasmonic Waveguide (HPWGs) [11], where plasmon and dielectric guiding leads the guiding mechanism [12,13]. The general layout of the HPWGs, which require three media, is shown in Figure 1. The high-index medium (Semiconductor) is positioned between the conducting medium (Metal) and low-index medium (Dielectric) [11]. The hybrid plasmonic waveguide can be used to design different passive and active devices such as multiplexers, combinational circuits, modulators, logic gates, resonators, hybrid plasmonic waveguides, filters, couplers, switches, converters, splitters, flip flop circuits nanocavities [14,15]. Flip-flop circuits are essential in a digital system used in communication and computer networks.



http://doi.org/10.30684/etj.2023.142434.1532
Received 11 August 2023; Received in revised form 29 November 2023; Accepted 07 December 2023; Available online 16 March 2024
2412-0758/University of Technology-Iraq, Baghdad, Iraq

In this research, the D and T-flip flop based on HPWGs was designed at 1310 nm operating wavelength and 30% transmission threshold (Tthreshold). Because of its exceptional optical transparency and improved toughness, aluminum oxynitride (ALON), AlN-$Al_2O_3$, is employed as a semiconductor material [16].

The proposed circuit has 400 nm × 400 nm dimensions, incorporating square-shaped nano-ring resonators and strips. The configuration of this research is as follows: Section 2 shows the network setup and theoretical concept. Section 3 shows the results and discussions of system design, and section 4 discusses the conclusion.

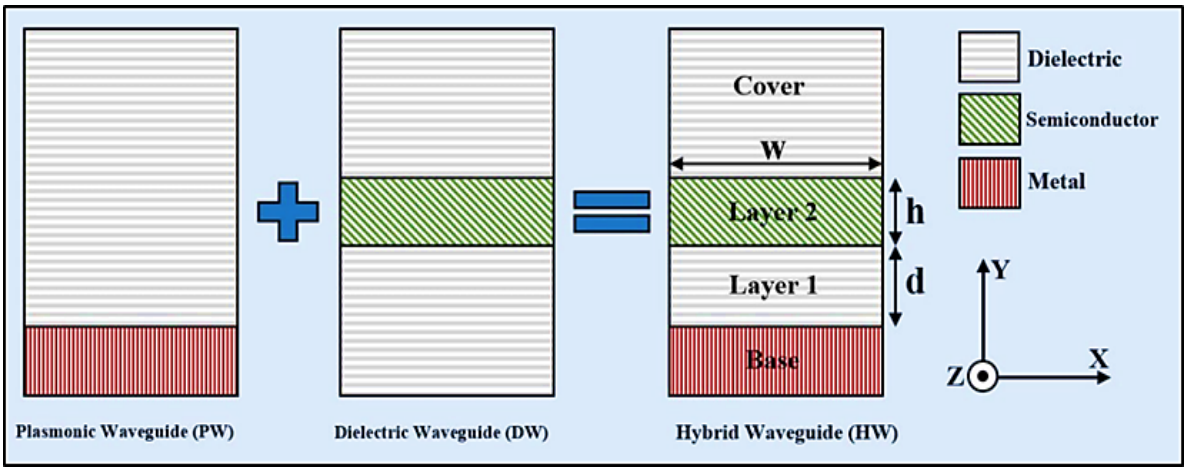


**Figure 1:** Fundamental format of HPWGs [11]

## 2. Theoretical Concept and System Setup

The hybrid plasmonic waveguide is a multilayer system. In our design, the system consists of Teflon as a dielectric material with ($\varepsilon_{Teflon}$) and silver ($\varepsilon_{Ag}$) as a conducting material. A high-index semiconductor material having ($\varepsilon_{ALON}$) is ALON. For theoretical analysis, let us assume the structure in Figure 1 with the materials we mentioned for propagation in the Z direction, the magnetic field $\overrightarrow{H_q}(y,z)$ for layers q=1 and q=2 is as follow [11]:

$$\overrightarrow{H_q}(y,z) = H_{xq}(y)exp\ (j(\beta_z - \omega t))\hat{x} \tag{1}$$

where $\beta$ is the complex propagation constant, which is equivalent to $k_\circ(n_{eff} + jk_{eff})$, $k_\circ$ is the wavenumber given by $(\frac{2\pi}{\lambda_\circ})$, $t$ is time. The real $n_{eff}$ and the imaginary $k_{eff}$ are the two major characteristics of the effective refractive index.

$$\overrightarrow{H_{Cover}}(y,z) = A_c\ exp\left(-k_c\big(y-(d+h)\big)\right) ex\,p\big(j(\beta_z - \omega t)\big)\,\hat{x} \tag{2}$$

$$\overrightarrow{H_{Base}}(y,z) = A_b\ exp(k_b y)\ exp\ (j(\beta_z - \omega t))\hat{x} \tag{3}$$

Equations 2 and 3 [11] expressed the magnitude of the magnetic field in the cover $\overrightarrow{H_{Cover}}(y,z)$ and base $\overrightarrow{H_{Base}}(y,z)$ and represented by $A_c$ and $A_b$, respectively. $k_c$ and $k_b$ are the attenuation rates for the cover and base layers, respectively, and they are equal to [11]:

$$K_{Base} = \sqrt{(\beta^2 - \varepsilon_{Ag}k_\circ^2)} \tag{4}$$

$$K_{Cover} = \sqrt{(\beta^2 - \varepsilon_{Teflon}k_\circ^2)} \tag{5}$$

$\varepsilon_{Teflon}$ is the dielectric constant of the metal, $\varepsilon_{Ag}$ is the dielectric constant of the insulator. Figure 2 depicts the layout suggested for achieving the D- and T-flip flops using the HPW. The configuration consists of three straight lines, three rectangle-shaped elements for silver, two square ring resonators, two straight lines for the ALON material, and the remaining elements for Teflon. As seen in Figure 2, there are four ports; three of them have been located as entrance ports, namely, input, previous, and clock, and the fourth as output ports following the requirements of the hybrid plasmonic flip flops. TM-polarized plane waves are fired for the input, previous, and clock ports to excite surface waves.

The data from Hartnett et al. [16] was used to demonstrate ALON's permittivity, while Johnson and Christy's data [17] proposed the permittivity of silver. Additionally, for Teflon material, the refractive index is 1.375 [11]. To calculate the resonance condition for rectangle ring resonators [18]:

$$L = m\left(\frac{\lambda_{resonance}}{ReN_{eff}}\right) \qquad m = positive\ integer \tag{6}$$

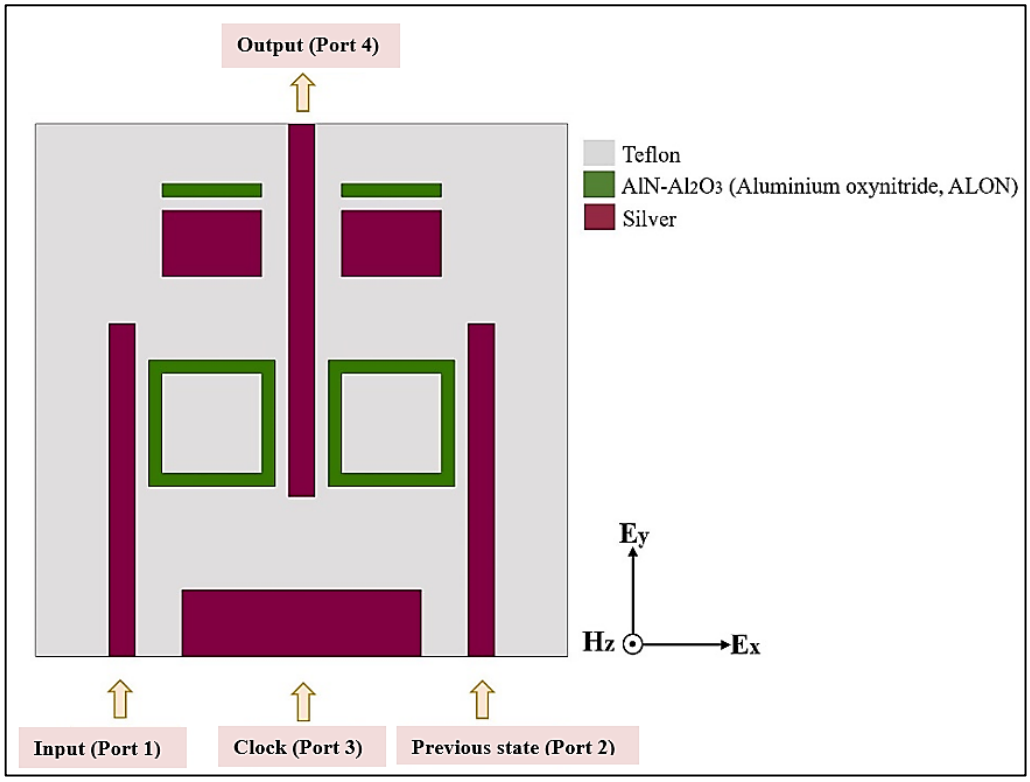


**Figure 2:** Structure of the D-flip flop and T-flip flop

*L* is the square's total length, m is the number of integer modes, and $N_{eff}$ is the effective refractive index. The material's type and the dimensions of the structure are two crucial factors in determining the system's resonance wavelength. The D-flip flop and T-flip flop's performance was evaluated using four criteria. The first assesses the ratio of output optical power to the input power at a single port (input or control port), called transmission value (T). To distinguish between two states at a single port, the $T_{threshold}$ are chosen to be 30% to achieve two flip flops in the same structure.

$$T = P_{out}/P_{input} \tag{7}$$

where $T$ is the transmission value, $P_{out}$ and $P_{input}$ are the output and input power, respectively [19]. The second criterion is the Contrast Ratio (CR), which is the relationship between the smallest signal power for the ON state and the greatest optical signal power for the OFF state [20]:

$$CR = 10\log(P_{out}|ON)min\ /(P_{out}|OFF)max \tag{8}$$

Is the suggested design's dimension producing the greatest results? The Modulation Depth (MD), the third criterion, provides an answer to this query [21]:

$$MD = (T_{ON}|max - T_{OFF}|\min\ )T_{ON}max \tag{9}$$

where $T_{OFF}|\min$ is the smallest transmission in the OFF-state condition, $T_{ON}|max$ is the largest transmission in the ON-state condition.

The Insertion Loss (IL) in dB is the fourth criterion, defined as the loss in signal power from the input port to the minimum transmission of the output port in the case of ON state [22].

$$IL = 10\log(P_{out}|\mathrm{ON})\,min/(P_{in}) \tag{10}$$

The concept of constructive and destructive interferences between the input light signal(s) and control light signal(s) relies on the phase of the incoming light wave and the location of the input port(s) and control port(s) if all other factors (configuration, size, dimensions of the structure, and materials utilized) stay constant. When the phase of the incident wave of the ports (including the control port) and the propagation direction (depending on the location of the ports) are the same, constructive interference occurs. In contrast, destructive interference occurs when the phase or direction of the propagation of the incident wave of the ports is different [23]. According to the Equation in [11]:

$$u = \left(4N_{eff}b_m cos\theta\right)/\lambda_{incident} \tag{11}$$

The effective refractive index of silver is $N_{eff}$, the thickness of the metal is $b_m$, the incident wave's phase is $\theta$, and the wavelength of the incident light is $\lambda_{incident}$. Here, $u$ is the interference order as an integer greater than zero.

The sign of Equation 11 is positive when $\theta = 0^{\circ}$. This indicates that the mode propagates in the same direction as the wave. Consequently, constructive interference develops between modes with the same phase. Hence, the transmission will be boosted. The sign of Equation 11 is positive when $\theta = 45^{\circ}$. This indicates that the mode propagates in the same direction as the wave. Thus, constructive interference occurs with modes with the same phase, but its magnitude is smaller than when $\theta = 0^{\circ}$. As a consequence, the transmission will be raised slightly. When θ is 90 degrees, Equation 11 equals zero. Hence, no constructive nor destructive interference will occur in this mode. Depending on the other phases of input(s) and control of light waves, the transmission either increases or decreases in addition to the other factors. The sign of Equation 11 is negative when $\theta = 180^{\circ}$.

This indicates that the mode propagates in the opposite direction of the light wave. Furthermore, destructive interference develops across modes with different phases. Accordingly, the transmission will be reduced. Therefore, the function of each proposed hybrid plasmonic circuit is determined by the phase of the incoming light wave and by the assessment of the proposed structure ports (which are an input port(s), a control port(s), and an output port(s)).

The truth table of the D-flip flop and T-flip flop are shown in Tables 1 and 2, respectively [24].

**Table 1:** Truth table of the D-flip flop

| D input | Previous state (Q) | Next state ($Q^+$) |
|---|---|---|
| 0 | 0 | 0 |
| 0 | 1 | 0 |
| 1 | 0 | 1 |
| 1 | 1 | 1 |

**Table 2:** Truth table of the T-flip flop

| T input | Previous state (Q) | Next state (Q+) |
|---|---|---|
| 0 | 0 | 0 |
| 0 | 1 | 1 |
| 1 | 0 | 1 |
| 1 | 1 | 0 |

## 3. Results and Discussion

The transmission behavior at the required wavelength (1310 nm) is modified (maximized or minimized) by altering the metal employed in the suggested structure, while all other parameters remain identical.

It becomes unattractive in some metals (i.e., Ti and Hg). Figure 4 depicts the proposed structure's metal. As demonstrated in Figure 2, silver material is the optimal option for the suggested design owing to its transmission characteristics at 1310 nm.

By altering the dielectric employed in the suggested construction while leaving all other parameters fixed, the transmission characteristics will be shifted to the right or left relative to the intended wavelength. Figure 5 depicts the dielectric material utilized in the suggested construction. Teflon material, with a refractive index of 1.375 and a resonance wavelength of 1310 nm, is the better decision for the dielectric that has to be employed in the suggested construction. It can be noted, that all structure dimensions are in nanometer scale as shown in Figure 3.

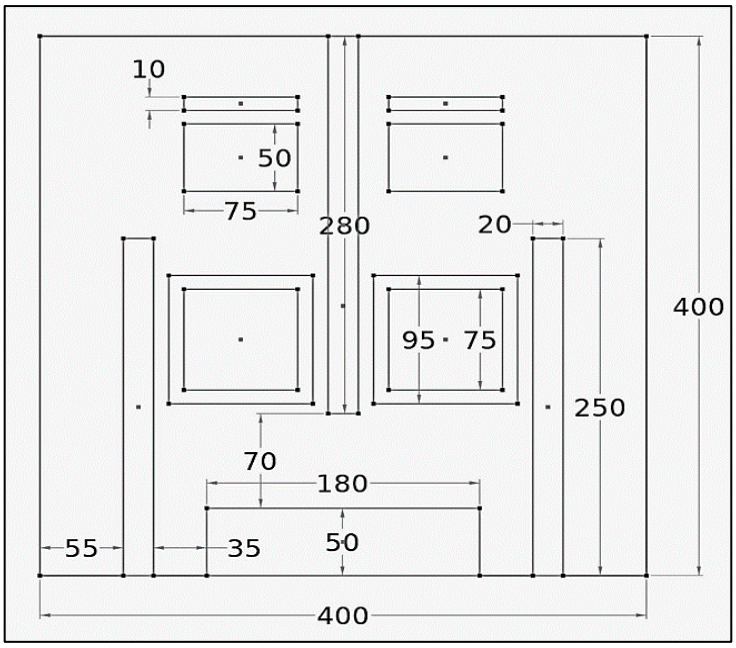


**Figure 3:** Dimensions of the HPWG structure all in (nm)

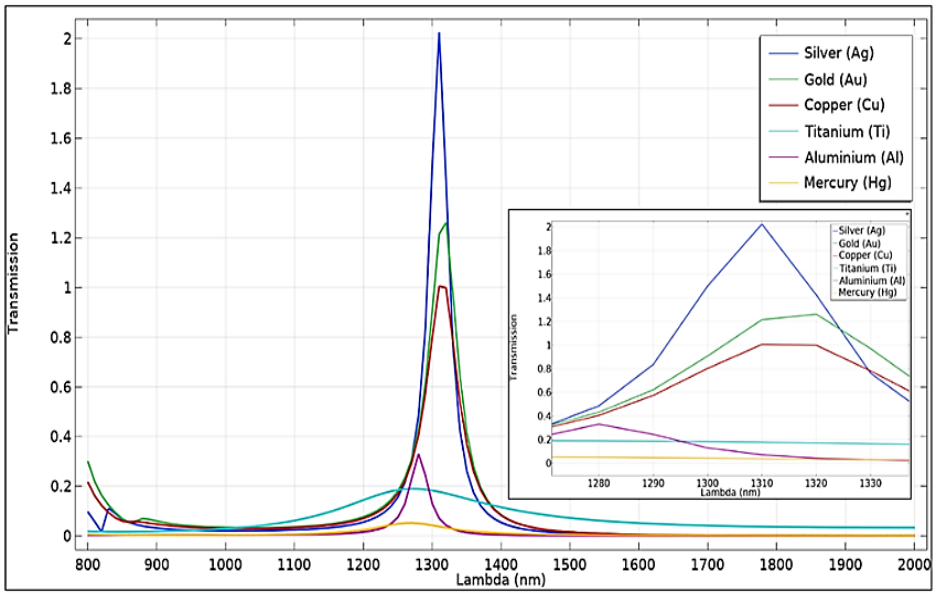


**Figure 4:** Effectiveness of the metal utilized in the submitted configuration

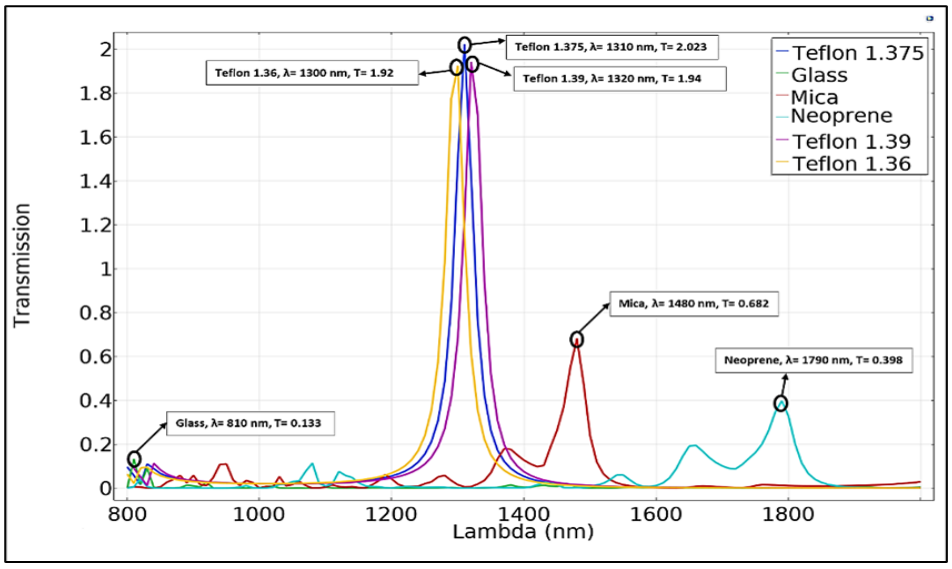


**Figure 5:** Effectiveness of the dielectric utilized in the submitted configuration

The transmission behavior with the desired wavelength (1310 nm) is altered, maximized, or minimized with slight shifting to the right or left and becomes unacceptable in certain materials (e.g., Indium arsenide (InAs)) whenever the semiconductor material employed in the offered structure is changed, while all other parameters remain unchanged. The semiconductor utilized in the submitted structure is shown in Figure 6. Aluminum oxynitride (ALON) is the optimal semiconducting material for the proposed design owing to its transmission performance at 1310 nm.

Changing the side length of the inner square ring resonator in the proposed construction would affect transmission even when all other parameters stay fixed. The transmission's intensity will vary. When the inner side length is below 75 nm, it will drop slightly. When the inner side length is more than 75 nm, the resonance wavelength also shifts somewhat relative to the desired wavelength. Figure 7 depicts the inner side length of the square ring of the suggested construction.

Suppose the side length of the outer square ring resonator in the suggested construction is more than 95 nm. In that case, the transmission will reduce, and the resonance wavelength will shift to the right while all other parameters stay identical. When the outer side length of the resonator is smaller than 95 nm, transmission similarly declines, but by a different proportion, and the resonance wavelength shifts to the left. Figure 8 depicts the outer side length of the suggested structure's square resonator. The resonator's optimal outer side length value is 95 nm, resulting in a resonance wavelength of 1310 nm.

In the suggested structure, if the length of the side stripes is less than 250 nm and all other parameters stay the same, the resonance wavelength will be displaced to the left with a reduction in transmission. When the length exceeds 250 nm, the resonance wavelength will have moved to the right, and the transmission magnitude will also decrease. Figure 9 depicts the side strip length of the designed construction. The side strip length employed in the suggested structure is 250 nm, making the optimal transmission achieved in the resonance wavelength of 1310 nm.

The transmission value changes (increases and decreases) by a minor percentage when the width of the side stripes is altered in the proposed construction, with all other parameters held constant. When the width is less than 20 nm, the resonance wavelength shifts to the left. When the width exceeds 20 nm, the wavelength of resonance shifts to the right. Figure 10 illustrates the stripe width of the suggested structure. The optimal stripe width in the suggested system is 20 nm, resulting in a maximum transmission with a resonance wavelength of 1310 nm.

The length of the center stripe was determined to be 280 nm based on the curves shown in Figure 11. The transmission magnitude is the most significant variable that may be influenced by stripe length. It reduces or rises with a very small ratio but remains below the T value associated with the central stripe length of 280 nm. In contrast to what was accomplished with the side stripes, the length change does not cause any shift in the resonance wavelength.

On the other hand, the resonance wavelength is affected by the central stripe's varying width. When the width is less than 20 nm, the resonance wavelength shifts to the left as the transmission's magnitude increases, while when the width is greater than 20 nm, the resonance wavelength shifts to the right as the transmission decreases. The optimal value for the width of the central stripe is 20 nm because the resonance wavelength reaches 1310 nm with sufficient transmission magnitude, as shown in Figure 12. In summary, depending on the size, parameters of the proposed structure, materials and refractive index of the chosen materials, the port position, and the phase of the incident field, the transmission of the optical power is minimized or maximized.

The effectiveness of the metal used, dielectric, semiconductor, and structure parameters concerning transmission behavior have been demonstrated.

The HPW used in the structure of Figure 2 to implement the flip flops had been struck by incident waves for the input ports in the case of ON-state to achieve the functionality of the D-flip flop and T-flip flop in the same structure for a wavelength of 1310 nm.

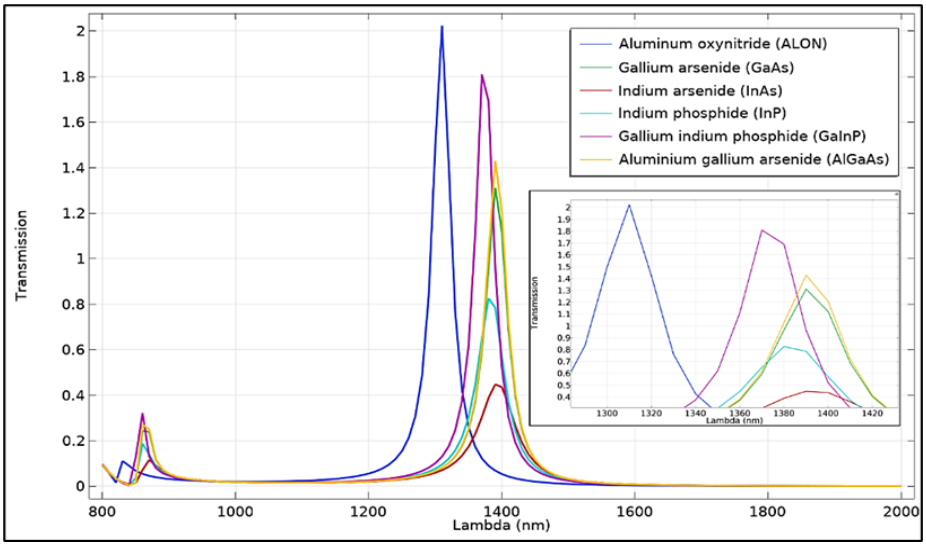


**Figure 6:** Effectiveness of the semiconductor utilized in the offered structure

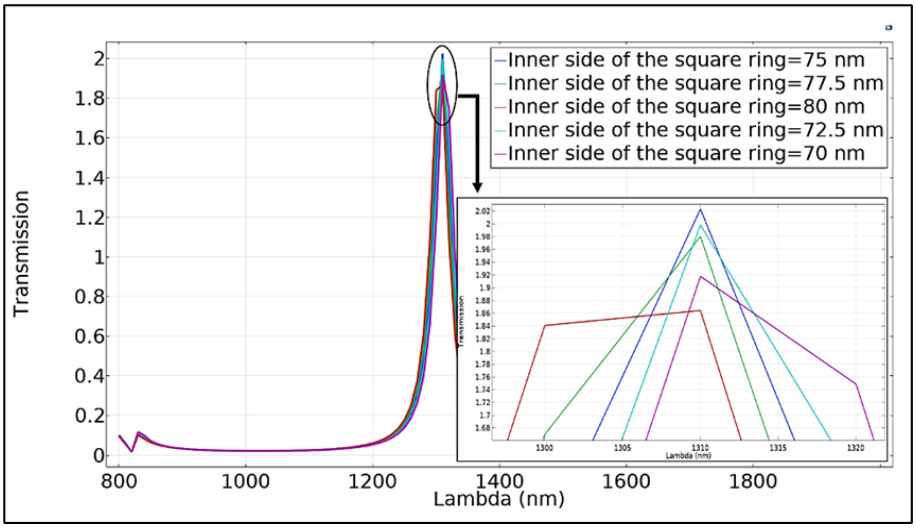


**Figure 7:** Effectiveness of the inner side of the square ring for the suggested system

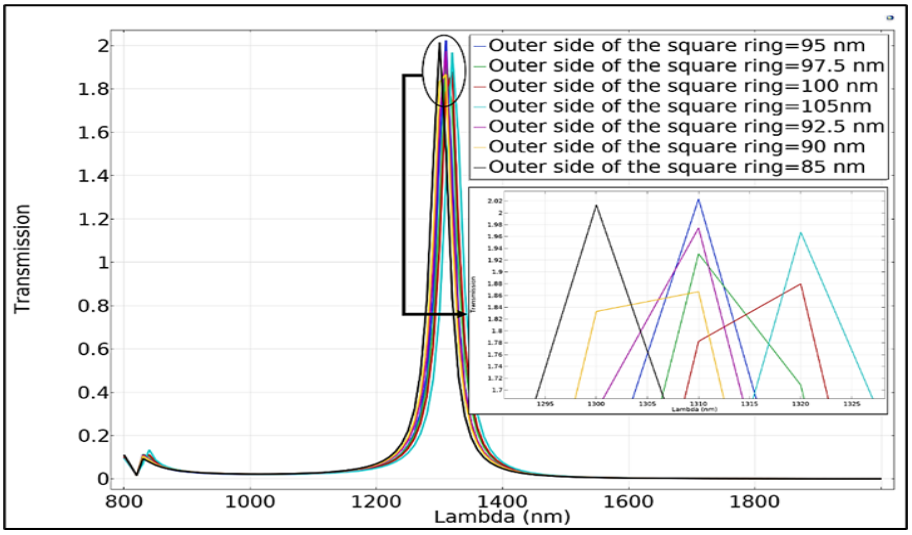


**Figure 8:** Effectiveness of the outer side of the square ring for the suggested system

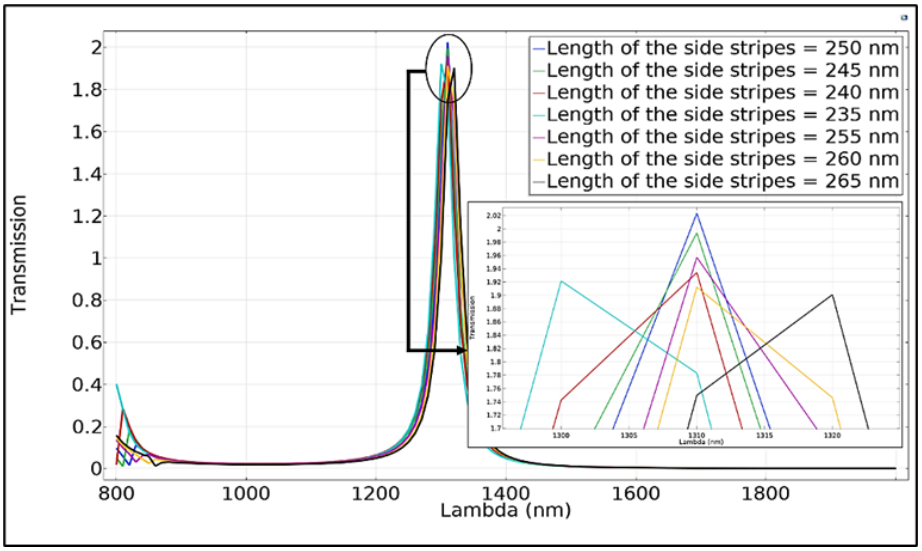


**Figure 9:** Effectiveness of the length of the side stripes for the proposed system

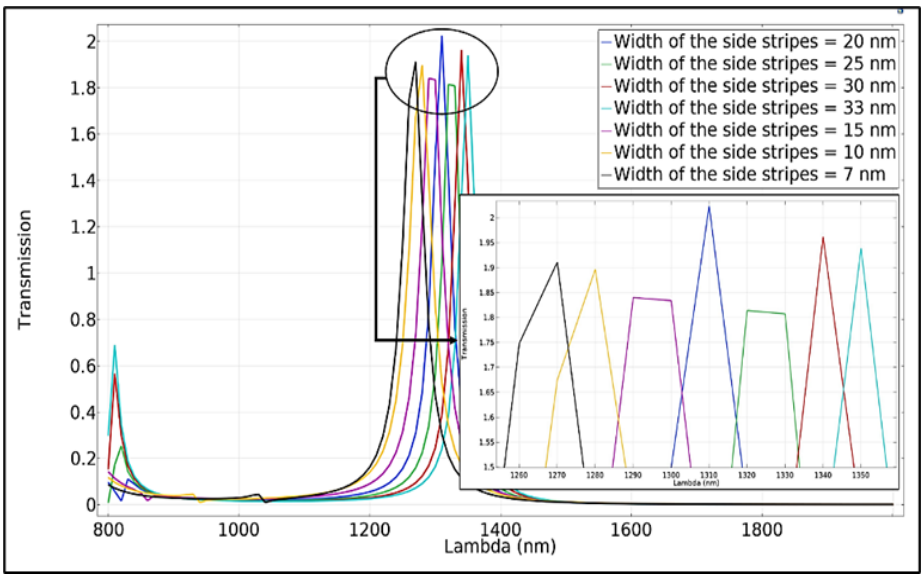


**Figure 10:** Effectiveness of the width of the side stripes for the proposed system

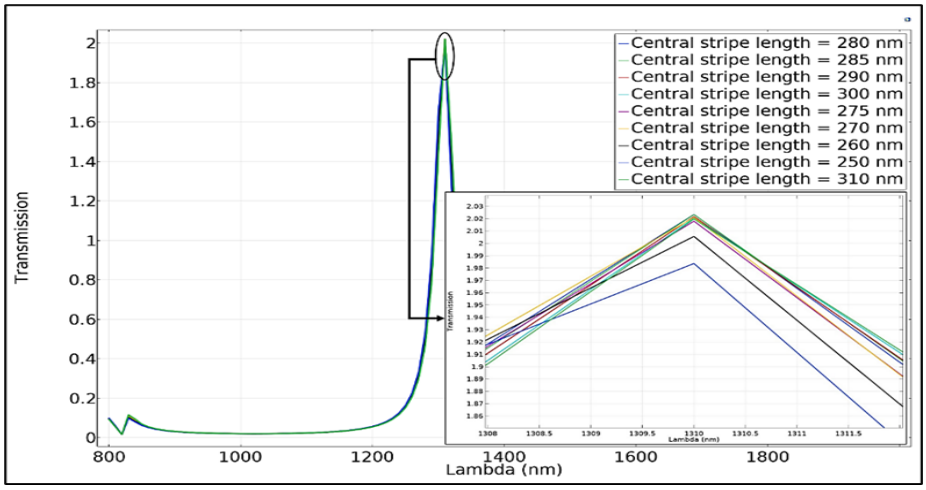


**Figure 11:** Effectiveness of the length of the central stripe for the proposed system

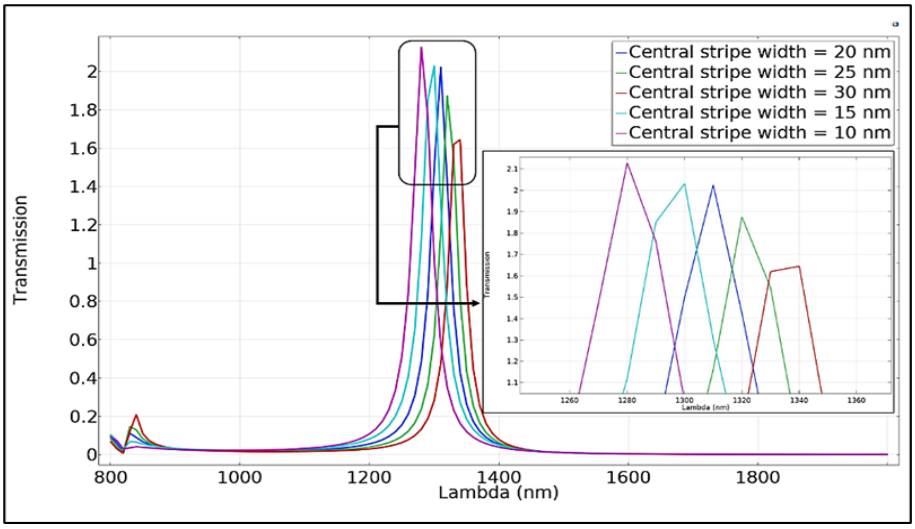


**Figure 12:** Effectiveness of the width of the central stripe for the proposed system

## 3.1 Hybrid plasmonic D and T-flip flops

The D and T-flip flop configuration states that port 1 represents the input port (D or T input), port 2 occupies the previous state (Q), port 3 simulates the clock permanently active, and port 4 is the output port.

The output of the D-flip flop (next state (Q+)) provides logic 1 whenever the D-input is ON. Table 3 shows the probabilities between the D-input port and the previous state port Q in the presence of the clock. A constructive interference means that the phase shift between the D-input port and the previous state port Q is 0° leading to a transmission value greater than the Tthreshold, which is 30%. The T values are 2.023 and 0.723 for ON-ON and ON-OFF states, respectively.

If the D input has a logic 0, the output of the flip flop will be OFF. For example, in the OFF-ON state, as listed in Table 3, a destructive interference occurred between the previous state port Q, which is in this case (ON), and the clock port (always ON), causing the phase shift difference to be 180°. The resultant power ratio at the output is below the Tthreshold (13% out of 30%).

Now we can notice that the last case in Table 3 comes with a Transmission value of 2.023, which is an amplification effect because, logically, no transmission value will exceed 100 % at the output port; the reason behind that is the effect of the square disk resonator near the output port for both sides of our design, the disk resonator that resonates at only single frequency which is 1310 nm used to enhance the transmission and that what distinguishes it from the ring resonator. The reflection of the surface waves at that resonator with the condition of ($m\ \lambda_{SPP}$) makes constructive interferences inside the disk resonator. In the resultant, the transmission value exceeds 100 % and equals 202.3%.

**Table 3:** The proposed hybrid D-flip flop's transmission values

| Inputs | | Input P1 | Previous (Q) P2 | Clock P3 | T value | Output (Q+) |
|---|---|---|---|---|---|---|
| 0 | 0 | OFF (0°) | OFF (0°) | ON (0°) | 0.047/0.3 | 0 |
| 0 | 1 | OFF (0°) | ON (180°) | ON (0°) | 0.13/0.3 | 0 |
| 1 | 0 | ON (0°) | OFF (0°) | ON (0°) | 0.723/0.3 | 1 |
| 1 | 1 | ON (0°) | ON (0°) | ON (0°) | 2.023/0.3 | 1 |

Table 4 describes the aspects that evaluate the performance of the suggested flip-flops; the value of the CR is calculated according to Equation 8 , and in our D, the Flip-flop is equal to 7.45 dB. This value indicates that the variance between the lowest ON-state and the highest OFF-state is moderate [11], which means the circuit will operate correctly.

On the other hand, the MD value is greater than 90%, which pointed out that the circuit is operated excellently and optimally from the point of view of the selected dimension, and the port position fits our design [11] as the formula of the insertion losses in [22]. It is clear that the negative value indicates a loss in a particular port (output port) because the value is in (dB). As it is a power ratio, that means when the signal arrives at the output port, The amount of power decreases by a certain percentage if we compare it with that of the input port, so the result of dividing the power at the output port by that at the input port would be less than one, taking the logarithmic scale for this value make it in negative, but how much the negative value? If it's a small value, that means low insertion loss; if it is a high negative value, that means a high amount of insertion loss. On the other side, according to the formula of the insertion loss, the positive value means that the power at the output port is higher than the input port due to the amplification effect of the hybrid plasmonic waveguides, so the value will be positive. CR, MD, and IL of the D-flip flop are displayed in Table 4. The offered curves of the transmission spectrum versus wavelength and the electric field distribution of the structure are shown in Figures 13 and 14, respectively.

**Table 4:** Computations of the different criteria for the presented hybrid D-flip flop

| Output Power (μW) | | CR | MD | IL |
|---|---|---|---|---|
| $P_{Min}$ \|*ON* | $P_{Max}$ \|*OFF* | | | |
| 0.723 | 0.13 | 7.45 dB | 97.67 % | -1.4 dB |

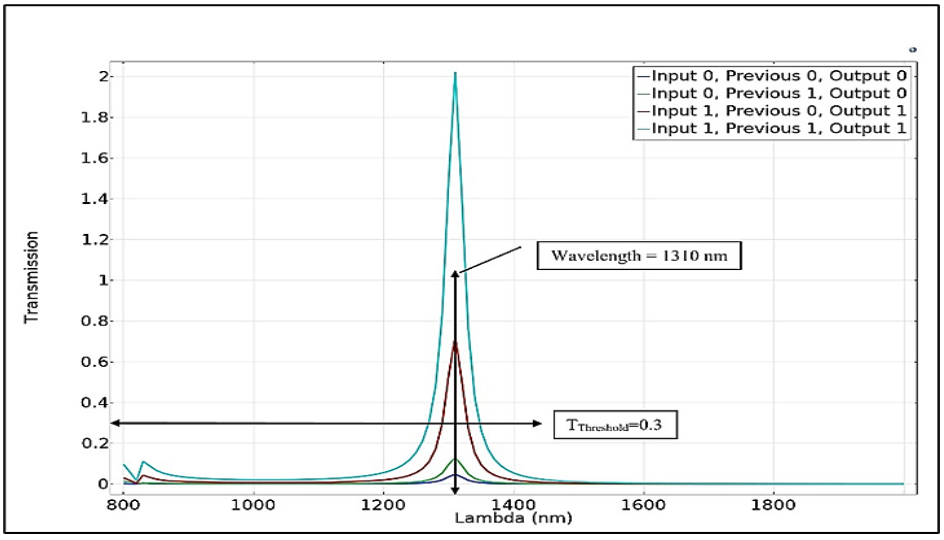


**Figure 13:** Shows the proposed hybrid D-flip flop's power ratio spectrum

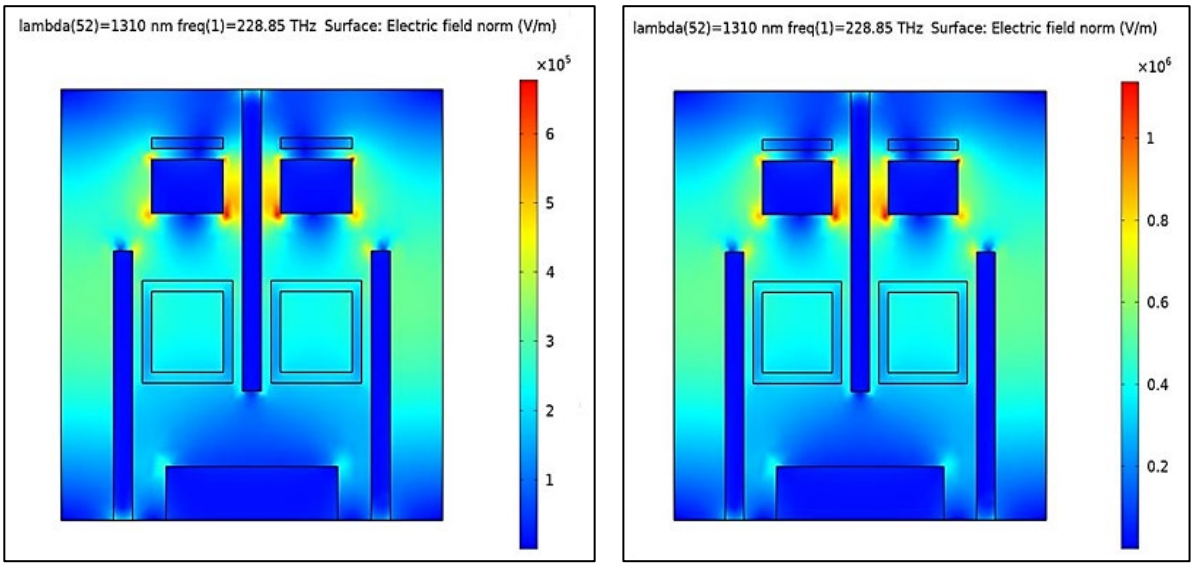


**(a)** **(b)**

**Figure 14:** Distribution of the electric field for the D-flip flop (a) 1 0 state (b) 1 1 state

In T flip flop, When the T-input port and the previous state port Q have opposite levels (OFF-ON) or (ON-OFF), the phase difference between the two ports is 0°; more specifically (the phase shift between the clock port and the active port from the mentioned ports is 0°) this leads to constructive interference, and the power ratio is greater than the Tthreshold, the output of the T-flip flop offers a logic 1. On the other hand, the T-flip flop output is OFF if the T-input and previous state Q ports have the same levels.

In the case of the ON-ON state, for example, destructive interference is caused by the phase difference between the clock port and the mentioned ports, causing the output to be in the OFF state. Table 5 lists all of the T values for the recommended T-flip flop. Table 6 shows the T-flip flop's CR, MD, and IL weights. The curves of the transmission spectrum versus wavelength and the electric field distribution of the structure are shown in Figures 15 and 16, respectively.

**Table 5:** The proposed hybrid T-flip flop's transmission values

| Inputs | | Input P1 | Previous (Q) P2 | Clock P3 | T value | Output (Q+) |
|---|---|---|---|---|---|---|
| 0 | 0 | OFF (0°) | OFF (0°) | ON (0°) | 0.047/0.3 | 0 |
| 0 | 1 | OFF (0°) | ON (0°) | ON (0°) | 0.62/0.3 | 1 |
| 1 | 0 | ON (0°) | OFF (0°) | ON (0°) | 0.723/0.3 | 1 |
| 1 | 1 | ON (0°) | ON (180°) | ON (90°) | 0.034/0.3 | 0 |

**Table 6:** Computations of the different criteria for the presented hybrid T-flip flop

| Output Power (μW) | | CR | MD | IL |
|---|---|---|---|---|
| $P_{Min}$ \|*ON* | $P_{Max}$ \|*OFF* | | | |
| 0.62 | 0.047 | 11.2 dB | 95.29 % | -2.07 dB |

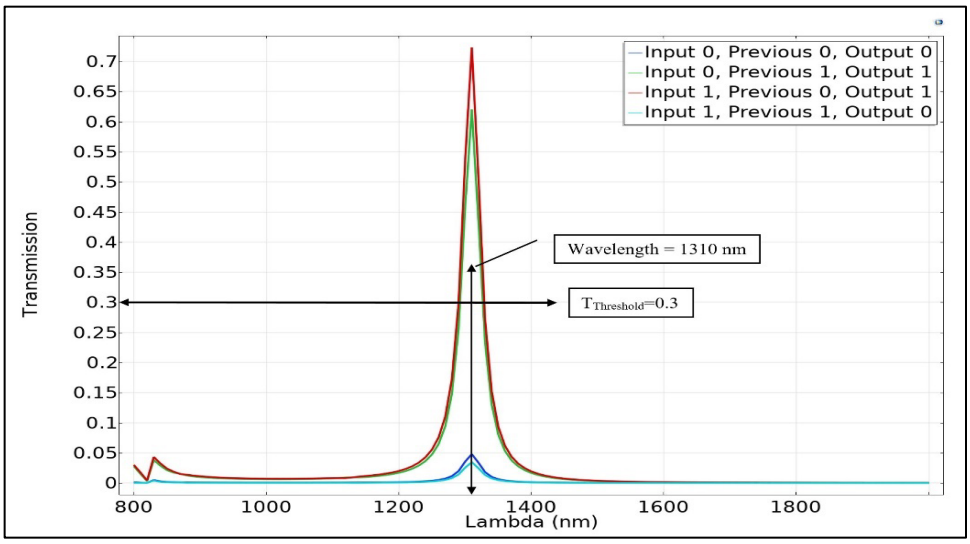


**Figure 15:** Shows the proposed hybrid T-flip flop's power ratio spectrum

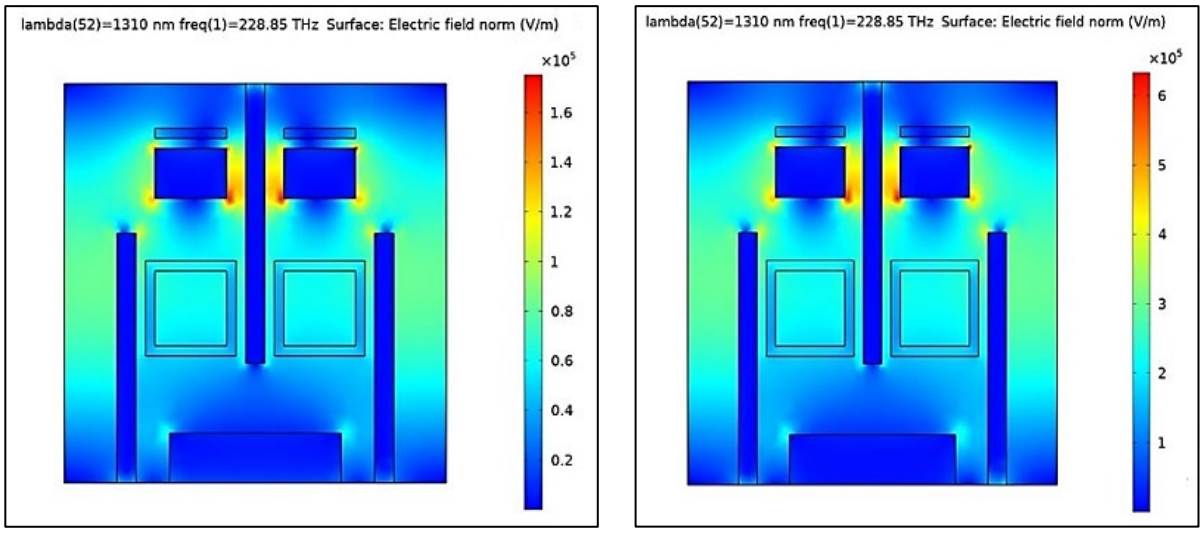


**(a)** **(b)**

**Figure 16:** Distribution of the electric field for the T-flip flop (a) 0 0 state (b) 0 1 state

In Table 7, a comparison between this design and other previous designs is presented. When the other researchers suggested only one form of the flip-flop, we simulated and studied D and T flip-flops in the same structure. Our structure has dimensions of 400 nm × 400 nm, an operating wavelength of 1310 nm, and a transmission threshold equal to 30%. The other structures have dimensions in micrometer scales at 1550 nm [25] and 12.8 µm [10] operating wavelengths. While just CR is suggested for the first research and three criteria (Transmission, CR, and IL) are suggested for the second research, four alternative criteria (Transmission, CR, MD, and IL) were proposed to discuss the performance of our design.

The insertion loss for T and D flip-flops in our system is -2.07 dB and -1.4 dB, while the insertion loss for D flip-flops in the competing design is 0.087 dB [25].

**Table 7:** Proposed Comparator versus Previous Systems

| Criteria | This work | [10] | [26] |
|---|---|---|---|
| Software | FEM | FDTD | FDTD |
| Proposed structure | Square- shaped nano-ring (HPWGs) | Graphene-based plasmonic waveguides | photonic crystal waveguides, T-shaped waveguides |
| Number of circuits | 2 Sequential Logic Functions | 1 | 1 |
| Proposed circuits | D- Flip Flop<br>T-Flip Flop | SR Flip Flop | D Flip Flop |
| Size | 400 nm × 400 nm | 1.62 µm$^2$ | 6 8.4 × 5.4 µm$^2$ |
| Wavelength | 1310 nm | 12.8 µm | 1550 nm |
| Dielectric | Teflon | *** | Silicon rods in Air |
| Nobel metal | Silver | | |
| Semiconductor | Aluminum Oxynitride | | |
| Performance | Transmission, CR, MD, and IL | CR | Transmission, CR, and IL |
| Tthreshold ON/OFF | 30% | *** | *** |

## 4. Conclusion

This work demonstrates a new structure that uses hybrid plasmonic waveguides to carry out optical D and T flip flops. The resonance wavelength, chosen in this work to be 1310 nm, was defined by the nature of the material used and the size of the structure. Several optical applications make use of that critical window. The phase shift between the incoming light waves that strike the system ports, the constructive and destructive interferences among these signals, and the locations of the ports in the suggested structure can cause an increase or decrease in the transmission value at the output ports. The transmission threshold can be used to recognize both ON and OFF states. The transmission threshold value is selected to be 30%. The CR, MD, and IL criteria were proposed to describe the system performance. The CR are 7.45 dB and 11.2dB, respectively, for the D and T flip flop, and the MD is 97.67 % and 95.2 for the D and T flip flop. Finally, the IL is -1.4 dB and -2.07dB for the D and T flip flop. In future work, the design of a hybrid plasmonic waveguide can be used to design other digital components such as modulators, multiplexers, couplers, and splitter.

### Author contributions

Conceptualization, S. Abdulwahid, A. Wadday, and S. Abdul Satta; methodology, S. Abdulwahid; software, S. Abdulwahid; validation, S. Abdulwahid; formal analysis, S. Abdulwahid; investigation, S. Abdulwahid; writing—original draft preparation, S. Abdulwahid ; review and editing, A. Wadday, and S. Abdul Sattar; supervision, A. Wadday, and S. Abdul Sattar; project administration, A. Wadday, and S. Abdul Sattar. All authors have read and agreed to the published version of the manuscript.

### Funding

This research received no specific grant from any funding agency in the public, commercial, or not-for-profit sectors.

### Data availability statement

The data that support the findings of this study are available on request from the corresponding author.

### Conflicts of interest

The authors declare that there is no conflict of interest.

## References

**[1]** M. J. Maleki, M. Soroosh, and G. Akbarizadeh, A subwavelength graphene surface plasmon polariton-based decoder, Diam. Relat. Mater., 134 (2023) 1–11, https://doi.org/10.1016/j.diamond.2023.109780

**[2]** D. G. S. Rao, V. Palacharla, S. Swarnakar, and S. Kumar, Design of all-optical D flip-flop using photonic crystal waveguides for optical computing and networking, Appl. Opt., 59 (2020) 7139. https://doi.org/10.1364/AO.400223

**[3]** A. Dolatabady and N. Granpayeh, All-optical logic gates in plasmonic metal–insulator–metal nanowaveguide with slot cavity resonator, J. Nanophotonics, 11(2017) 026001. https://doi.org/10.1117/1.JNP.11.026001

**[4]** A. Kumari, A. Pal, A. Singh, and S. Sharma, All-optical binary to gray code converter using non-linear material based MIM waveguide, Optik, 200 (2020) 163449. https://doi.org/10.1016/j.ijleo.2019.163449

**[5]** S. H. Abdulwahid, A. G. Wadday, and S. M. Abdulsatar, Design of Optical Combinational Circuits Utilized with Hybrid Plasmonic Waveguides, Plasmonics, 18 (2023) 9–28. https://doi.org/10.1007/s11468-022-01733-5

**[6]** S. H. Abdulwahid, M. R. Saeed, and A. A. Hadi, Design of three-bit binary to gray converter based on metal–insulator–metal plasmonic waveguides, Appl. Opt., 62 (2023) 6456–6463. https://doi.org/10.1364/AO.500028

**[7]** S. H. Abdulwahid, A. G. Wadday, F. M. Ali, B. J. Hamza, and A. N. Al-Shamani, Realization of an optical nanostructure 4× 1 multiplexer based on metal-insulator-metal plasmonic waveguides, Appl.Opt., 62 (2023) 6163–6168. https://doi.org/10.1364/AO.497810

**[8]** H. Falah Fakhruldeen, Design and Simulation of All-Optical Plasmonic Logic Gates Based on Nano-Ring Insulator-Metal-Insulator Waveguides, Int. J. Advanc. Sci. Technol., 29 (2020) 405-424. https://doi.org/10.26782/jmcms.2020.02.00015

**[9]** H. K. Al-Musawi, A. K. Al-Janabi, S. A. W. Al-abassi, N. A. H. A. Abusiba, and N. A. H. Q. Al-Fatlawi, Plasmonic logic gates based on dielectric-metal-dielectric design with two optical communication bands, Optik, 223(2020) 165416, https://doi.org/10.1016/j.ijleo.2020.165416

**[10]** M. H. Rezaei and A. Zarifkar, "Graphene-based plasmonic electro-optical SR flip-flop with an ultra-compact footprint," Opt Express, 28(2020) 25167. https://doi.org/10.1364/OE.398597

**[11]** S. H. Abdulwahid, A. G. Wadday, and S. M. A. Sattar, New structure for an all-optical logic gate based on hybrid plasmonic square-shaped nano-ring resonators and strips, Opt Quantum Electron., 54 (2022) 1–23. http://dx.doi.org/10.1007/s11082-022-04018-7

**[12]** A. A. Alwahib, S. M. Hasan, and K. A. Hubeatir, A surface plasmon temperature sensor based on E7 liquid crystal using angle interrogation method, J. Electromagn. Waves Appl., 36(2021) 1–15. https://doi.org/10.1080/09205071.2021.1960901

**[13]** H. A. A. Abdul Amir, M. A. Fakhri, and A. Alwahib, Synthesized of GaN Nanostructure Using 1064 nm Laser Wavelength by Pulsed Laser Ablation in Liquid, Eng.Technol.J., vol. 40 (2022) 404–411. https://doi.org/10.30684/etj.v40i2.2271

**[14]** M. Z. Alam, J. S. Aitchison, and M. Mojahedi, Theoretical analysis of hybrid plasmonic waveguide, IEEE Journal of Selected Topics in Quantum Electronics, 19 (2013) 4602008. https://doi.org/10.1109/JSTQE.2013.2238894

**[15]** D. Dai and S. He, A silicon-based hybrid plasmonic waveguide with a metal cap for a nano-scale light confinement, Opt. Express, 17 (2009) 16646–16653. https://doi.org/10.1364/OE.17.016646

**[16]** M. Fujii, J. Leuthold, and W. Freude, Dispersion relation and loss of subwavelength confined mode of metal-dielectric-gap optical waveguides, IEEE Photonics Technol. Letters, 21 (2009) 362–364. https://doi.org/10.1109/LPT.2008.2011995

**[17]** T. M. Hartnett, S. D. Bernstein, E. A. Maguire, and R. W. Tustison, Optical properties of ALON (aluminum oxynitride), Infrared Physics Technol., 39 (1998)203-211. https://doi.org/10.1016/S1350-4495(98)00007-3

**[18]** P. B. Johnson and R.-Wjp. Christy, Optical constants of the noble metals, Phys. Rev. B, 6 (1972) 4370. https://doi.org/10.1103/PhysRevB.6.4370

**[19]** X. Peng, H. Li, C. Wu, G. Cao, and Z. Liu, Research on transmission characteristics of aperture-coupled square-ring resonator based filter, Opt Commun., 294 (2013) 368–371. https://doi.org/10.1016/j.optcom.2012.12.026

**[20]** Y.-D. Wu, Y.-T. Hsueh, and T.-T. Shih, Novel All-optical Logic Gates Based on Microring Metal-insulator-metal Plasmonic Waveguides, PIERS Proceedings, (2013) 169-172.

**[21]** M. N. Abbas and S. H. Abdulnabi, Plasmonic reversible logic gates, J. Nanophotonics, 14 (2020) 016003. https://doi.org/10.1117/1.JNP.14.016003

**[22]** S. H. Abdulnabi and M. N. Abbas, All-optical logic gates based on nanoring insulator–metal–insulator plasmonic waveguides at optical communications band, J. Nanophotonics, 13 (2019) 016009.https://doi.org/10.1117/1.JNP.13.016009

**[23]** S. H. Abdulwahid, A. G. Wadday, and S. M. A. Sattar, All-optical design for multiplexer and comparator utilizing hybrid plasmonic waveguides, Appl. Opt., 61 (2022) 8864–8872. https://doi.org/10.1364/AO.474373

**[24]** S. H. Abdulnabi and M. N. Abbas, Design an all-optical combinational logic circuits based on nano-ring insulator-metal-insulator plasmonic waveguides, Photonics,6 (2019) 30. https://doi.org/10.3390/photonics6010030

**[25]** T. L. Floyd, Digital fundamentals: A systems approach, Pearson Education Limited, 2014.

**[26]** D. G. S. Rao, V. Palacharla, S. Swarnakar, and S. Kumar, Design of all-optical D flip-flop using photonic crystal waveguides for optical computing and networking, Appl. Opt., 59 (2020) 7139-7143. https://doi.org/10.1364/ao.400223.